Site-Directed Mutagenesis and Use of Bile Acid−MTS Conjugates to Probe the Role of Cysteines in the Human Apical Sodium-Dependent Bile Acid Transporter (SLC10A2)†

Antara Banerjee,‡ Abhijit Ray,‡ Cheng Chang,§ and Peter W. Swaan*,‡

Department of Pharmaceutical Sciences, University of Maryland, 20 Penn Street, Baltimore, Maryland 21201

Received March 25, 2005; Revised Manuscript Received April 29, 2005

ABSTRACT: The residues involved in substrate interaction of the human apical sodium-dependent bile acid transporter (hASBT, SLC10A2) remain undefined. Biochemical modification of conserved cysteine residues has suggested their direct involvement in hASBT function. In the present study, we developed novel methanethiosulfonyl (MTS)−bile salt derivatives and describe their reactivity toward hASBT and its mutants. Endogenous Cys residues were subjected to Ala/Thr scanning mutagenesis and subsequent exposure to affinity inactivators. We show that C51A/T, C105A/T, C144A, and C255A/T are loss-of-function mutations. Additionally, C74A/T cell surface expression was abolished suggesting a role in protein folding and/or trafficking. C270A remained largely unaffected in the presence of 1.0 mM polar and charged MTS reagents (MTSEA, MTSES, and MTSET) and retained function similar to wt-hASBT control. However, in the presence of synthetic cholyl− and chenodeoxycholyl−MTS analogues, C270A displayed a significant decrease in K_T and J_{max}. Our findings demonstrate that Cys270 is a highly accessible extracellular residue susceptible to thiol modification in its native form that remains largely unaffected upon mutation to Ala. Consequently, C270A provides an ideal scaffold for cysteine scanning mutagenesis studies. Furthermore, the substantial decrease in ligand affinity and maximal transport capacity of C270A suggest that C270 may potentially impact, although not critically, a putative substrate binding domain of hASBT. Overall, bile acid−MTS conjugates can serve as novel and powerful tools to probe the role of endogenous as well as engineered Cys residues and, ultimately, aid in defining their role in the bile acid binding region(s) of hASBT.

The apical sodium-dependent bile acid transporter (ASBT) belongs to a family of Na^+/bile acid cotransporters that are critical to the enterohepatic circulation of bile acids. Human ASBT (hASBT)[1] is a 348 amino acid, 41 kDa glycoprotein, coded in approximately 4 kb mRNA species (*1*), and hydropathy analysis predicts seven to nine putative transmembrane domains (*2*−*4*). Because of its unique substrate specificity and pivotal role in cholesterol homeostasis, ASBT has been targeted for drug delivery stratagems and has received increasing attention as a potential pharmacological target for the treatment of hypercholesterolemia (*5*, *6*).

To gain an understanding into the transport mechanism of hASBT, it is imperative to map the location of ligand binding site(s). However, in the absence of a high-resolution structure of this transporter protein, presently no direct information is available regarding the amino acid residues forming its ligand binding domain(s). One approach that can yield information regarding the solvent accessibility of residues in putative ligand binding domains is the "substituted cysteine accessibility method" (SCAM) (*7*). This technique determines the reactivity of native Cys residues and, along with cysteine-scanning mutagenesis, has provided keen insights into the translocation pathway of various transport proteins (*8*, *9*). SCAM studies generally require a Cys-less mutant to simplify interpretation; however, it has proven unfeasible to generate a functionally active Cys-less hASBT mutant. Early studies using thiol modifying agents (*10*) suggested the possible involvement of Cys residues in ASBT−ligand interactions, and ligand protection assays further confirmed the presence of Cys residues in the vicinity of the bile acid binding region(s). Thiol groups have also been found essential in murine ASBT (*11*) as well as in Na^+/taurocholate (NTCP) uptake by rat hepatocytes (*12*, *13*). hASBT comprises 13 endogenous cysteines, 12 of which are conserved among other mammalian species (Figure 1) (*2*). On the basis of a 7 transmembrane (TM) model, (*3*) seven cysteines are localized extracellularly (Figure 2); of these, C270 has been suggested to lie within the substrate binding region (*14*).

† This research was supported by a grant from the National Institutes of Health, National Institute for Digestive Diseases and Kidney DK061425 (to P.W.S).

* Corresponding author: Peter W. Swaan, Ph.D., University of Maryland, 20 Penn Street, HSF2-621, Baltimore, MD 21201. Tel:, 410-706-0103; fax, 410-706-1590; e-mail, pswaan@rx.umaryland.edu.

‡ University of Maryland.

§ Present address: Biophysics Program, The Ohio State University, Columbus, OH 43210.

[1] Abbreviations: MTSET, [2-(trimethylammonium)ethyl]-methanethiosulfonate; MTSEA 2-(Aminoethyl)methanethiosulfonate hydrobromide; CDCA, chenodeoxycholic acid; CA, cholic acid; hASBT, Human apical sodium-dependent bile acid transporter; IBAT, Ileal bile acid transporter; MTSES, methanethiosulfonate ethylsulfonate; Ntcp, sodium taurocholate cotransporting polypeptide; TCA, taurocholic acid; TM, transmembrane.

10.1021/bi050553s CCC: $30.25
Published on Web 05/26/2005

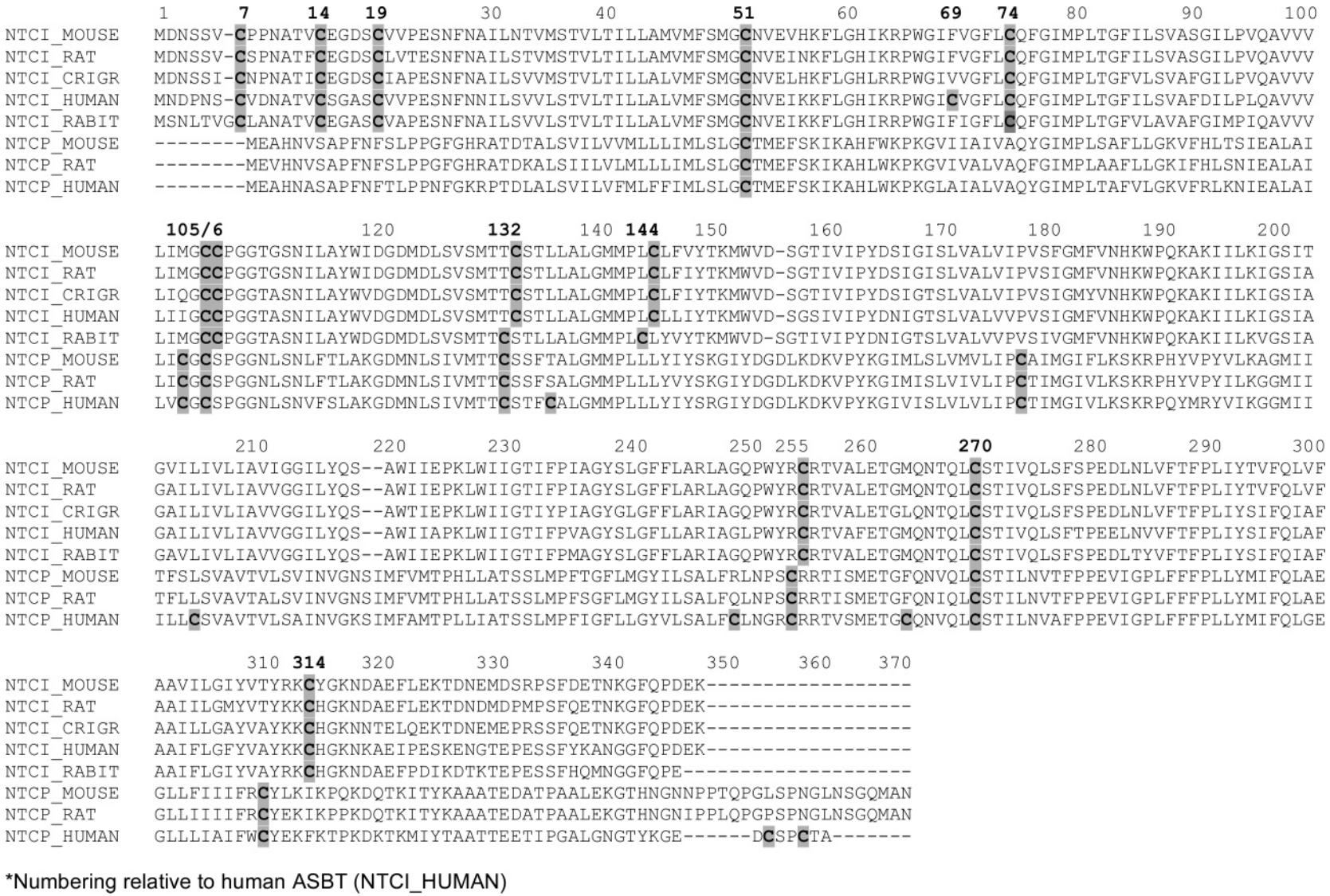

FIGURE 1: Multiple protein sequence alignment of ASBT (*SLC10A2*). Protein sequences were retrieved from GenBank in FASTA format and aligned via the MULTALIN routine. Annotation was performed with the program MPSA. NTCI, Na^+ taurocholate cotransporter ileum (ASBT, SLC10A2); NTCP, Na^+ taurocholate cotransporting polypeptide (hepatic, SLC10A1); CRIGR, hamster

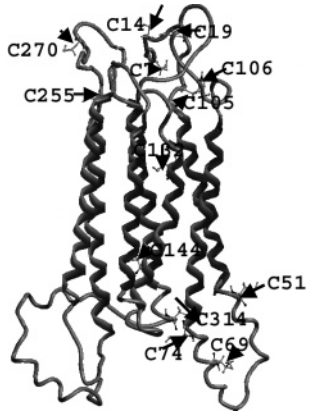

FIGURE 2: Model for the three-dimensional structure of hASBT consisting of 7 TM domains. Numbering of these domains is counterclockwise viewed from the extracellular side analogous to the numbering of the TM regions of bacteriorhodopsin. The model was generated using SYBYL 6.9. The TM domains are represented in line ribbons and the loops with tubes. The 13 cysteine residues have been represented in ball-and-stick and are numbered based on their location according to the 7 TM model of hASBT.

The reactivity of Cys residues can be probed by thiol-reactive methanethiosulfonate (MTS) analogues. For example, MTS-verapamil and MTS-rhodamine have been successfully used to define the drug-binding site of P-glycoprotein (*15*, *16*). Furthermore, MTS-galactose/glucose derivatives have been used for probing the catalytic mechanism of the *Escherichia coli* lactose permease (*17*). The objective of the current study was to probe the functional significance of endogenous Cys residues in hASBT using site-directed mutagenesis in conjunction with previously designed MTS−bile acid conjugates (Scheme 1). If the Cys

Name	Structure
MTSEA	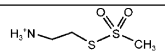
MTSES	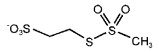
MTSET	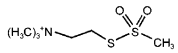
Allyl-MTS	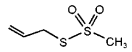

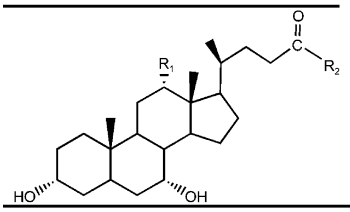

	$-R_1$	$-R_2$
Cholic Acid (CA)	-OH	-OH
CA-MTS	-OH	$-NHCH_2CH_2SSO_2CH_3$
CA-Asp-MTS	-OH	-Asp- $NHCH_2CH_2SSO_2CH_3$
CDCA-Asp-MTS	-H	-Asp- $NHCH_2CH_2SSO_2CH_3$

residues are in a critically functional region (s), the changes in charge-to-mass ratio as a result of covalent modification with MTS-analogues may obstruct ligand translocation, thereby aiding in the identification of critical Cys residues. In the present study, we show that extracellular Cys residue C270 has unique properties and that its alanine mutant (C270A), in conjunction with appropriate MTS−bile acid analogues, may serve as a suitable platform for future SCAM studies.

MATERIALS AND METHODS

Materials. ^{3}H-Taurocholic acid (50 Ci/mmol) was purchased from American Radiolabeled Chemicals, Inc. (St. Louis, MO). Sulfo-NHS-LC biotin was purchased from Pierce Biotech (Rockford, IL). MTS reagents MTSEA, MTSES, MTSET, and Allyl-MTS were purchased from Toronto Research Chemicals, Inc. (North York, ON, Canada). Taurocholic acid, cholic acid, and chenodeoxycholic acid were purchased from Sigma (St. Louis, MO). All other reagents and chemicals were of highest purity available commercially. Oligonucleotides for mutagenesis studies were custom synthesized and purchased from Invitrogen Life Technologies (Rockville, MD).

*Synthesis of Bile Acid−MTS Conjugate*s. Synthesis of methanethiosulfonic acid *S*-{2-[4-(3,7,12-trihydroxy-10,13-dimethyl-hexadecahydro-cyclopenta[a]phenanthren-17-yl)-pentylamino]-ethyl} ester (CA-MTS) was carried out by the activation of the carboxyl group in cholic acid to the *N*-hydroxysuccinimidyl group which was subsequently reacted with MTSEA to give the desired product. The synthesis of *N*-(2-methanesulfonylsulfanyl-ethyl)-2-[4-(3,7,12-trihydroxy-10,13-dimethyl-hexadecahydro-cyclopenta[a]phenanthren-17-yl)-pentanoylamino]-succinamic acid (CA-Asp−MTS) and 2-[4-(3,7-dihydroxy-10,13-dimethyl-hexadecahydro-cyclopenta[a]phenanthren-17-yl)-pentanoylamino]-*N*-(2-methanesulfonyl sulfanyl-ethyl)succinamic acid (CDCA-Asp−MTS) were synthesized by reacting boc-L-aspartic acid-4-*tert*-butyl 1-(hydroxysuccinimide) ester with MTSEA and the resultant product with activated (*N*-hydroxysuccinimidyl) CA or CDCA to give the desired products (Scheme 1). The formation of the final products was confirmed by high-resolution mass spectroscopy.

Cell Culture. The monkey kidney fibroblast cell line, COS-1 (CRL-1650) was obtained from ATCC (Manassas, VA). Cells were grown and maintained in Dulbecco's modified Eagle's Medium containing 10% fetal calf serum, 4.5 g/L glucose, 100 units/mL penicillin, and 100 μg/mL streptomycin (Life Technologies, Inc., Rockville, MD) at 37 °C in a humidified atmosphere with 5% CO_2.

Site-Directed Mutagenesis and Transient Transfection. The hASBT cDNA in the pCMV5 vector (kindly provided by Dr. Paul Dawson, Wake Forest University, Wisconsin-Salem, NC) was used as the template for all mutagenesis reactions. Site-directed mutations at each of the 13 cysteine residues to either alanine or threonine were introduced using the Quick Change Site-Directed mutagenesis kit from Stratagene (La Jolla, CA). All mutants were transformed into XL1 Blue strain of *E. coli*, amplified, and sequenced using a 3700 DNA analyzer (Applied Biosystems, Foster City, CA) at the Plant-Microbe Genomics Facility of the Ohio State University, Columbus, OH.

COS-1 cells were seeded at a density of 6×10^4 cells/mL on 24 well plates (Costar, Corning, NY) in antibiotic-free medium. Briefly, cells were transfected using the LipofectAmine PLUS reagent (Invitrogen, Carlsbald, CA).

Scheme 1

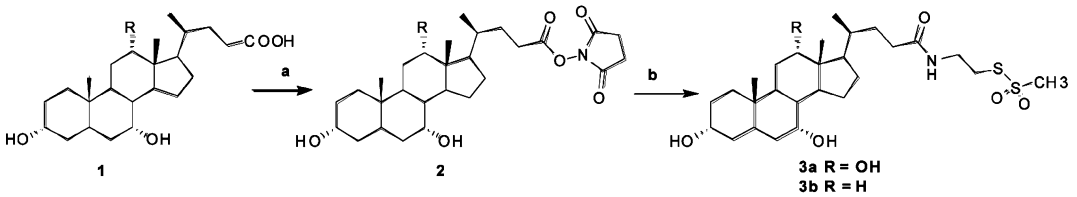

a. DMF, 1,4-Dioxane, H_2O, DIEA, TSTU; b. MTSEA:

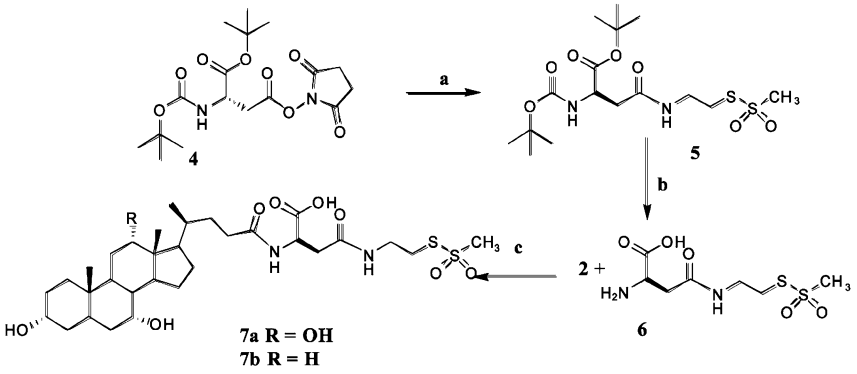

a. DMF; 1, 4-Dioxane; H_2O; DIEA; MTSEA: b. CH_2Cl_2; TFA; c. DMF; 1, 4-Dioxane; H_2O; DIEA:

Wild-type or mutant plasmid (400 ng/well) was diluted by DMEM, mixed with Plus Reagent, and incubated at room temperature for 15 min. The premixed DNA−PLUS solution was mixed with LipofectAmine reagent and allowed to incubate at room temperature for 15 min. The DNA−PLUS−LipofectAmine complex was then added to the cells and allowed to incubate for 5 h. The cells were used for subsequent uptake studies 48−72 h post-transfection (*3*).

Uptake Assay and Inhibition Studies. To determine the uptake activity, cells transfected with wt and mutant plasmids were used 48 h post-transfection. Transfected cells were washed two times with Dulbecco's PBS (DPBS, pH 7.4, 37 °C) containing Ca^{2+} and Mg^{2+} followed by incubation in uptake medium-modified Hanks' Balanced Salt Solution (MHBSS, pH 7.4) (*18*) at 37 °C, containing 5μM ^{3}H-taurocholic acid (TCA) (0.2Ci/mmol) for 12 min. Uptake was stopped by washing the cells four times in ice-cold DPBS, (pH 7.4) containing 0.2% fatty acid-free bovine serum albumin (BSA) and 0.5mM TCA. Cell-associated radioactivity was measured using an LS6500 liquid scintillation counter (Beckmann Coulter, Inc., Fullerton, CA) and normalized to total protein content, determined using the Bradford assay (Bio-Rad, Hercules, CA).

For inhibition studies, stock solutions of MTS reagents and bile acid−MTS conjugates were prepared in DMSO (final concentration $\leq$ 2%) and subsequently dispersed in uptake medium to obtain the desired experimental concentrations. Transfected cells were pretreated with 1 and 2.5 mM MTS analogues for 10 min at room temperature. Then, cells were washed twice with uptake medium and incubated with TCA (0−150 μM). Untreated controls (buffer only) were run in parallel. Cell viability was tested using the LIVE/DEAD assay (Molecular Probes Inc., Eugene, OR) as per the manufacturer's protocol.

Bile Acid Protection Assay. wt-hASBT COS-1 cells were treated with increasing concentrations of cholic acid (0, 5, 50, and 100μM) for 5 min prior to the addition of CA-Asp−MTS (1.0 mM). The cells were further incubated with the bile acid conjugate for 10 min, washed with uptake buffer, and equilibrated in MHBSS (pH 7.4, at 37 °C) for 15 min. Following equilibration, uptake kinetics was determined at increasing concentrations of TCA as described above.

Western Blot and Cell Surface Biotinylation. Protein expression of wt and mutant hASBT was determined by Western blot analysis as previously described (*3*). Briefly, cells were disrupted in lysis buffer (*10*), quantitated for total protein content, and resolved on a 10% Tris-HCl SDS−PAGE gel (Bio-Rad, Hercules, CA). Immunoblotting was carried out using a custom-prepared (*3*) rabbit anti-hASBT antibody (1:1000) and visualized using enhanced chemiluminescence (ECL plus, Amersham Bioscinces, Piscataway, NJ). β-Tubulin was used as a positive control in all the immuno assays. Densitometric analysis of the immunoreactive proteins were determined using the Bio-Rad Chemi Doc XRS system (Bio-Rad, Hercules, CA).

Cell surface expression of wt and mutant hASBTs was confirmed using the membrane-impermeant biotinylation reagent, Sulfo-NHS-LC Biotin (Pierce, Inc., Rockford, IL). Briefly cells were washed with PBS (pH 8.0) and incubated in PBS containing 0.5 mg/mL Sulfo-NHS-LC Biotin for 30 min at room temperature (*18*). Following several washes, cells were ruptured in lysis buffer containing 25 mM Tris, 300 mM NaCl, 1mM $CaCl_2$, and 1% Triton X-100 (pH 7.4) and centrifuged, and the supernatants were subjected to immunoprecipitation using anti-hASBT antibody and protein A-agarose. Following electrophoresis on a 10% SDS−PAGE gel and electroblotting, the final blots were blocked with 5% nonfat dry milk, followed by detection with anti-hASBT antibody. The specificity of the biotinylation reaction was verified by the fact that no band could be detected when COS-1 cells transfected with wt-hASBT and mutants were subjected to all labeling steps in the absence of Sulfo-NHS-LC-Biotin. To ensure that Sulfo-NHS-LC-Biotin is indeed a membrane impermeable reagent in our experimental

Table 1: PCR Primers for Preparing the Cys to Ala and Cys to Thr Mutants[a]

mutation	forward primer	reverse primer
C7A	GATCCGAACAGCGCCGTGGACAATGCAACAG	CTGTTGCATTGTCGGCACAGCTGTTCGGATC
C7T	GATCCGAACAGCACTGTGGACAATGCAAC	GTTGCATTGTCCACAGTGCTGTTCGGATC
C14A	CAATGCAACAGTTGCCTCTGGTGCATCCTG	CAGGATGCACCAGAGGCAACTGTTGCATTG
C14T	CAATGCAACAGTTACCTCTGGTGCATCCTG	CAGGATGCACCAGTGGTAACTGTTGCATTG
C19A	CTCTGGTGCATCCGCCGTGGTACCTGAGAG	CTCTCAGGTACCACGGCGGATGCACCAGAG
C19T	GCTCTGGTGCATCCACTGTGGTACCTGAG	CTCAGGTACCACAGTGGATGCACCAGAGC
C51A	GATGTTCTCCATGGGAGCCAACGTGGAAATC	GATTTCCACGTTGGCTCCCATGGAGAACATC
C51T	GATGTTCTCCATGGGAACCAACGTGGAAATC	GATTTCCACGTTGGTTCCCATGGAGAACATC
C69A	GGCCGTGGGGCATTGCTGTTGGCTTCCTC	GAGGAAGCCAACAGCAATGCCCCACGGCC
C69T	GGCCGTGGGGCATTACTGTTGGCTTCCTC	GAGGAAGCCAACAGTAATGCCCCACGGCC
C74A	GTTGGCTTCCTCGCTCAGTTTGGAATCATG	CATGATTCCAAACTGAGCGAGGAAGCCAAC
C74T	GTTGGCTTCCTCACTCAGTTTGGAATCATG	CATGATTCCAAACTGAGTGAGGAAGCCAAC
C105A	GTGCTCATTATAGGAGCCTGCCCTGGAGGAC	GTTCCTCCAGGGCAGGCTCCTATAATGAGCAC
C105T	GTGCTCATTATAGGAACCTGCCCTGGAGGAAC	GTTCCTCCAGGGCAGGTTCCTATAATGAGCAC
C106A	CTCATTATAGGATGCGCCCCTGGAGGAACTGCC	GGCAGTTCCTCCAGGGGCGCATCCTATAATGAG
C106T	CTCATTATAGGATGCACCCCTGGAGGAACTGCC	GGCAGTTCCTCCAGGGGTGCATCCTATAATGAG
C132A	GTCAGCATGACCACAGCCTCAACACTGCTTGC	GCAAGCAGTGTTGAGGCTGTGGTCATGCTGAC
C132T	GTCAGCATGACCACAACCTCAACACTGCTTGC	GCAAGCAGTGTTGAGGTTGTGGTCATGCTGAC
C144A	GGAATGATGCCGCTGGCCCTCCTTATCTATAC	GTATAGATAAGGAGGGCCAGCGGCATCATTCC
C144T	GGAATGATGCCGCTGACCCTCCTTATCTATAC	GTATAGATAAGGAGGGTCAGCGGCATCATTCC
C255A	CCCTGGTACAGGGCCCGAACGGTTGC	GCAACCGTTCGGGCCCTGTACCAGGG
C255T	CCCTGGTACAGGACCCGAACGGTTGC	GCAACCGTTCGGGTCCTGTACCAGGG
C270A	CAGAACACGCAGCTAGCTTCCACCATCGTTCAG	CTGAACGATGGTGGAAGCTAGCTGCGTGTTCTG
C270T	CAGAACACGCAGCTAACTTCCACCATCGTTCAG	CTGAACGATGGTGGAAGTTAGCTGCGTGTTCTG
C314A	GGCATACAAGAAAGCTCATGGAAAAAAC	GTTTTTTCCATGAGCTTTCTTGTATGCC
C314T	GTGGCATACAAGAAAACTCATGGAAAAAAC	GTTTTTTCCATGAGTTTTCTTGTATGCCAC

[a] Primers used to generate the cysteine to alanine and cysteine to threonine mutants. Amino acids are designated by single-letter code. For example, C7A represents the mutation of cysteine at position 7 to alanine.

protocol and specifically labels proteins on the cell surface, parallel studies were carried out followed by immunoprecipitation using anti-β-tubulin. No biotinylated β-tubulin could be detected (data not shown), whereas this abundant protein was easily detectable in control experiments with whole cell lysate.

Data Analysis and Statistics. All experiments were run in triplicate, and data are represented as mean ± SD. Nonlinear regression analysis was performed with GraphPad Prism 4.0 (San Diego, CA) using the Michaelis−Menten Equation $v = J_{max}C/(K_T + C)$, where v represents transporter velocity, J_{max} is the maximum transporter velocity, K_T is the concentration at half-maximal J_{max} and C is the substrate concentration. Statistical analyses within groups were performed using the unpaired Student's t test and between multiple groups using a one-way ANOVA, and data were considered statistically significant at $p \leq 0.05$.

RESULTS

Site-Directed Mutagenesis and Functional Activity of Ala and Thr Mutants. Thirteen endogenous cysteine residues are present in hASBT, 12 of which are conserved among ASBTs of other mammalian species (Figure 1) (*2*). Their relative positions along the polypeptide chain are shown in Figure 2. According to a 7 TM model, seven of these cysteines, C7, C14, C19, C105, C106, C255, and C270 would be situated in the extracellular face of the membrane, three (C74, C132, and C144) within the transmembrane region, and the remaining three cysteines (C51, C69, and C314) would lie within the cellular cytoplasm (Figure 2). C51, C105, C132, C255, and C270 are fully conserved residues in ASBT as well as its liver ortholog, NTCP (Figure 1). Each of the Cys residues were individually mutated to Ala and Thr (Table 1), resulting in several mutants with complete or significant loss of function (C51T, C74A, C74T, C105A, C105T, 255A/T, and C144A) (Table 2). While extracellular mutants C105A/T and C255A/T were inactive as a result of the mutation, the conversion of extracellular Cys residues at positions 7, 14, 19, and 106 to either Ala or Thr did not result in a significant loss of transporter activity (Table 2). These mutants retained greater than 65% activity compared to wt-hASBT. However, mutagenesis of C270 to Thr decreased its activity to 15% of wt. Interestingly, its alanine counterpart, C270A, maintained full transport activity (Table 2).

Table 2: ^{3}H−Taurocholate Uptake Activity of Cysteine Mutants[a]

mutation	activity (% of WT)	mutation	activity (% of WT)
beta[b]	7.09 ± 2.37	beta	2.14 ± 0.16
C7A	85.5 ± 9.4	C7T	131.9 ± 30.6
C14A	101.3 ± 20.6	C14T	76.5 ± 13.5
C19A	66.1 ± 1.6	C19T	149.8 ± 9.3 **
C51A	10.6 ± 1.8 **	C51T	2.7 ± 1.4
C69A	40.4 ± 6.0 **	C69T	44.2 ± 9.3 **
C74A	2.5 ± 0.6 **	C74T	2.6 ± 0.8 **
C105A	2.3 ± 0.6 **	C105T	3.6 ± 1.1 **
C106A	68.0 ± 8.8 *	C106T	10.6 ± 6.7 **
C132A	23.4 ± 11.3 **	C132T	15.5 ± 2.0
C144A	2.3 ± 0.4 **	C144T	84.0 ± 8.0
C255A	24.1 ± 8.3 **	C255T	9.6 ± 1.4 **
C270A	110.3 ± 8.6	C270T	6.2 ± 1.8 **
C314A	60.1 ± 6.0	C314T	73.0 ± 10.8

[a] Wild-type hASBT and cysteine mutants were expressed in COS-1 cells. Taurocholate uptake was measured at a concentration of 5 μM (0.2 Ci/mmol). Data are represented as mean ± SD of three to six measurements and are expressed as percent of mutant uptake relative to wild-type activity. [b] Beta is mock vector control. Significant decrease in uptake is indicated by "**" $p \leq 0.001$ and "*" $p \leq 0.01$

Uptake assays can quickly reveal the importance of a single mutant relative to wt activity; however, further characterization of transport kinetics is warranted for those mutants that have altered functionality other than loss-of-

Table 3: Kinetic Characterization of Cysteine Mutants in Presence and Absence of Bile Acid−MTS Conjugates[a]

	uptake buffer (MHBSS) pH 7.4		CA-Asp−MTS (1mM)	
	K_T (μM)	J_{max} pmol·min^{-1}·mg protein^{-1}	K_T (μM)	J_{max} pmol·min^{-1}·mg protein^{-1}
wt	11.1 ± 0.4	300.23 ± 8.3	72.2 ± 2.6 **	114.23 ± 10.2 **
C7A	21.8 ± 1.7*	83.84 ± 2.5 *	23.7 ± 2.4	71.93 ± 1.8
C14A	13.5 ±1.6	419.5 ± 1.0	19.7 ± 1.4	357.86 ± 8.8 **
C19A	14.3 ± 1.0	291.6 ± 1.7	16.1 ± 3.9	345.5 ± 24.5
C106A	7.3 ± 1.1 *	84.34 ± 5.9 *	7.7 ± 1.9	88.84 ± 4.9
C270A	17.1 ± 3.5	254.3 ± 12.3	9.12 ± 0.5 **	205.3 ± 5.9 **

[a] COS-1 cells were transfected with wt-hASBT and the Ala mutants. At 48 h post-transfection, cells were treated with 1 mM of CA-Asp−MTS for 10 min, followed by TCA uptake kinetics at increasing concentration from 0 to 150 μM (0.2 Ci/mmol). Data were fitted to the Micaelis−Menten equation and is represented as mean ± SD of three different measurements. Statistical differences in kinetic parameters between wt and mutants (*) and between wt and mutants in the presence and absence of bile acid−MTS conjugates (**) were considered significant with $p \leq 0.01$.

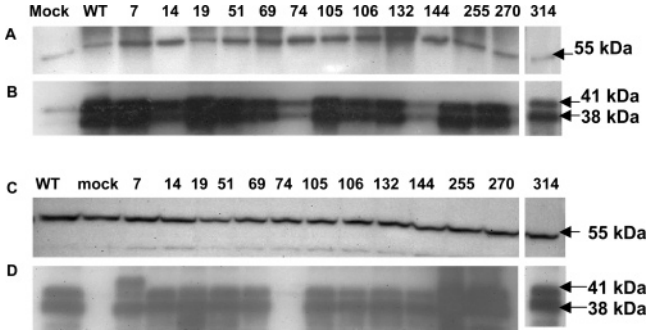

FIGURE 3: Cell surface biotinylation and Western blot analysis of the mutated hASBT transporter proteins expressed in COS-1 cells: COS-1 cells were transfected with Cys to Ala mutants (A and B) and Cys to Thr mutants (C and D). At 48 h post-transfection, the COS-1 cells were biotinylated with Sulfo NHS-LC Biotin for 30 min at room temperature and subjected to immunoprecipitation followed by Western blot analysis using affinity purified rabbit anti-hASBT primary antibody and were visualized using goat anti-rabbit HRP-conjugated secondary antibody. (B and D) Glycosylated (41 kDa) and unglycosylated (38 kDa) bands of hASBT were detected from the biotinylated samples. (A and C) Whole cell lysates of the COS-1 cells transfected with mutants were probed with anti-β-tubulin (55 kDa)

function mutants. Kinetic transport parameters of the extracellular Cys mutants revealed a significant decrease in J_{max} for C7A and C106A relative to wt-hASBT (Table 3), suggesting that lowered transport activity was directly attributable to the mutation. Altered substrate affinities due to the mutation were found to be less significant in case of C14A, C19A, and C270A, and only C14A displayed a significant increase in $J_{max.}$

Substitution of membrane-associated C132 as well as intracellular C69 and C314 reduced TCA accumulation, and this decrease in activity was not significantly affected by either Ala or Thr substitution (Table 2). C144A resulted in a loss-of-function mutant, but its activity was completely restored upon exchange to Thr. The loss of uptake activity for C144A could be attributed to the reduced plasma membrane expression of the mutant transporter as seen in Figure 3B. Plasma membrane insertion for the rest of the mutant transporters was confirmed by Western blot analysis and cell surface biotinylation; however, C74A/T showed little or no surface expression (Figure 3 B,D). Additionally, no protein expression in whole cell lysates was observed (data not shown).

C270A is a Fully Active Mutant that Renders ASBT Unreactive toward Charged MTS Reagents. The selection criterion for subsequent analysis of transporter kinetics was arbitrarily set at >50% of wt activity. Of the mutants that satisfied this requirement, five were located in the extracellular domain (C7A/T, C14A/T, C19A/T, C106A, and C270A). Even though C19T exhibits higher transport activity relative to C19A, we chose to use solely Ala-substituted mutants in our study to maintain uniformity and simplify data interpretation. It is particularly important to use both permeant and impermeant reagents to define the critical Cys residues. The well-characterized MTS reagents $MTSEA^+$, $MTSET^+$, $MTSES^-$, and Allyl-MTS (*19*) were selected to evaluate the function of the extracellular mutants C7A, C14A, C19A, C106A, and C270A. The polar molecules $MTSES^-$ and $MTSET^+$ are both membrane-impermeant, whereas $MTSEA^+$ and Allyl-MTS (a neutral molecule) are known to traverse the membrane to varying degrees (*20*). wt-hASBT is sensitive to all MTS reagents at 1.0 mM (Figure 4), and further inhibition of ligand uptake at 2.5 mM was insignificant (data not shown). Maximum inhibition of ligand uptake is observed with the partially permeable MTSEA and the fully permeable Allyl-MTS reagents. We would speculate that increased reactivity of wt-hASBT toward (semi)-permeable MTS modifiers could be attributed to the participation of membrane-bound or intracellular Cys residues.

Interestingly, C270A showed a significant increase in ligand uptake compared to wt control, and was relatively nonreactive toward polar MTS reagents. Even though C7A and C106A were also unaffected by the presence of MTS reagents, the overall ligand uptake caused by these mutations was significantly decreased compared to wt-ASBT. Hence, C270A displays unique properties not observed with other Cys mutants. C14A and C19A displayed differential responses to MTS reagents (MTSEA > MTSET) (Figure 4), but neither mutant was significantly affected by $MTSES^-$, which may indicate electrostatic repulsion of negatively charged MTS reagents at the site of MTS−ASBT interaction.

C270A Can Be Used as a Scaffold for Scanning the Bile Acid-Binding Domains with Bile Acid−MTS Conjugates. The unique characteristics and response of C270A to MTS reagents prompted us to further probe the location and role of this residue in h*ASBT*. This was facilitated by using custom-synthesized CA−MTS, CA-Asp−MTS, and CDCA-Asp−MTS. The initial rate of ^{3}H-TCA uptake was measured for wt-hASBT at varying concentrations of TCA at 137 mM Na^+ in COS-1 cells. Nonlinear regression analysis revealed a K_T of 11.1 ± 0.4 μM and a J_{max} of 300.2 ± 8.3 pmol·mg protein^{-1}·min^{-1} for wt-hASBT (Figure 5A). Following treatment with 1.0 mM MTSEA, the apparent affinity was

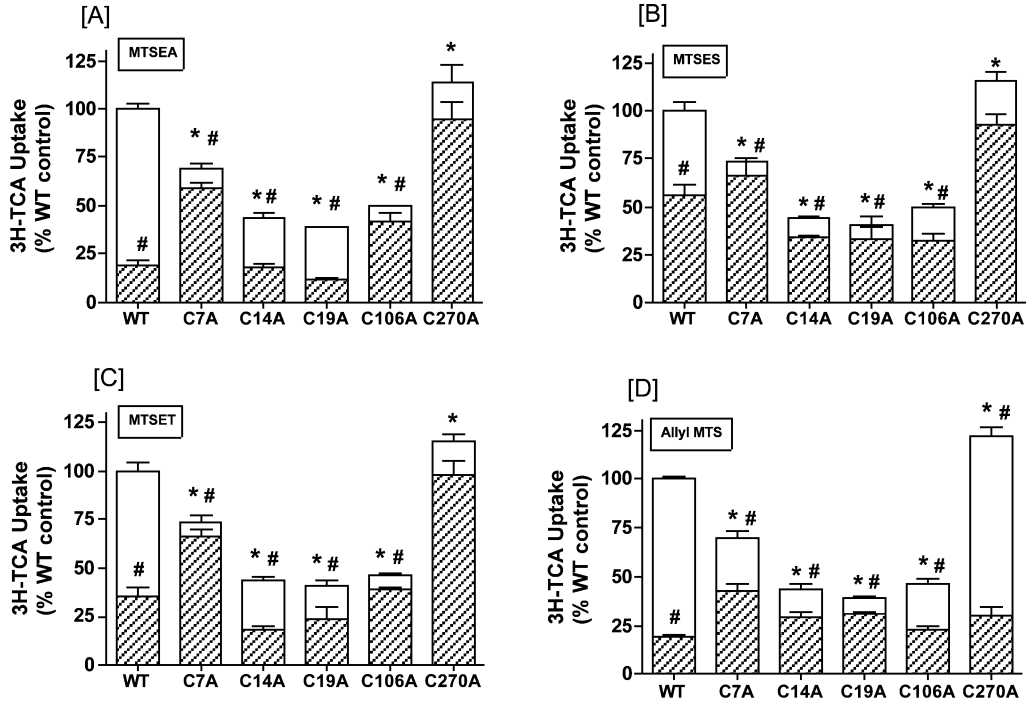

FIGURE 4: Effect of MTS reagents, MTSEA, MTSES, MTSET, and Allyl-MTS, on wild-type hASBT and Ala mutants: effect of MTS reagents were tested on WT and mutants C7A, C14A, C19A, C106A, and C270A. At 48 h post-transfection, the COS-1 cells were preincubated with buffer (open plus hashed *bars*) and 1mM (hashed bars) MTS reagents (A) MTSEA, (B) MTSES, (C) MTSET, and (D) Allyl-MTS for 10 min, followed by 5 μM ^{3}H-TCA (0.2 Ci/mmol) uptake at 37 °C for 12 min. In each case, cells treated with buffer alone were used as the control. Data are represented as percent of transport of the mutants relative to that of the wild-type as mean ± SD of three measurements. (*) Uptake (% control) was found to be statistically significant at $p \leq 0.05$. (#) Uptake (% control) in the presence of 1 mM MTS reagents was found to be statistically significant at $p \leq 0.05$.

significantly reduced ($p \leq 0.01$) to 17.0 ± 2.7 μM (Figure 5A), with a concurrent decrease in J_{max} of 140.3 ± 11.5 pmol·mg protein^{-1}·min^{-1}. Kinetic uptake parameters for C270A were also altered significantly from wt-hASBT (K_T, 17.3 ± 3.5 μM; J_{max}, 254.7 ± 12.3 pmol·mg protein^{-1}·min^{-1}). However, at 1.0 mM MTSEA, no further change in C270A uptake kinetics was observed (K_T, 20.7 ± 2.4 μM; J_{max}, 244.2 ± 3.2 pmol·mg protein^{-1}·min^{-1} vs buffer control). At higher MTSEA concentrations (10 mM), wt-hASBT activity was abolished, whereas C270A retained 40% activity, albeit with a significant loss in substrate affinity (K_T, 95.6 μM). Previous studies with C270A (*14*) did not observe a loss of activity in the presence of 10 mM MTSET and MTSES. We speculate that the effect of MTSEA at higher concentrations could be attributed to its concentration-dependent membrane permeability, thereby gaining more facile access to membranous or cytosolic Cys residues.

The most potent bile acid−MTS conjugate was CA−MTS (11% activity vs wt; Figure 5C). Its apolar nature may facilitate its movement through the lipid bilayer and, in turn, contribute to the sharp decrease in K_T, (69.9 μM) and J_{max} (35.8 pmol·mg protein^{-1}·min^{-1}). CA-Asp−MTS and CDCA-Asp−MTS exerted only ≤70% decrease in activity versus control (Figure 5C). Uptake of TCA in the presence of 1.0 mM CA−MTS, CA-Asp−MTS, and CDCA-Asp−MTS yields Michaelis−Menten-type kinetics (Figure 5C) with K_T values of 69.9 ± 4.5 μM, 72.2 ± 2.6 μM, and 11.2 ± 2.3 μM, respectively, and J_{max} values of 35.8 ± 0.3, 114.2 ± 10.2, and 122.7 ± 5.4 pmol·mg protein^{-1}·min^{-1}, respectively. Parallel studies with C270A demonstrated a 41% uptake activity with CA−MTS (K_T, 25.4 ± 3.1 μM; J_{max}, 134.3± 4.6 pmol·mg protein^{-1}·min^{-1}), 70% in the presence of CDCA-Asp−MTS (K_T, 11.56 ± 1.5 μM; J_{max}, 159.8 ± 0.9 pmol·mg protein^{-1}·min^{-1}), and as high as 85% in case the of CA-Asp−MTS (K_T, 9.2 ± 0.3 μM; J_{max}, 205.7 ± 5.9 pmol·mg protein^{-1}·min^{-1}) (Figure 5D), thus exhibiting a significant reduction in activity compared to its own control.

Asp−MTS was used as a negative control to demonstrate the specific interaction of bile acid−MTS conjugates with hASBT. This compound had no significant effect on transporter activity (wt, K_T 17.3 ± 2.3 and J_{max} 178.9 ± 11.4 pmol·mg protein^{-1}·min^{-1}; C270A, K_T 20.1 ± 3.0 and J_{max} 206.4 ± 18.6 pmol·mg protein^{-1}·min^{-1}) suggesting that the effect was due solely to Cys-selective modification of MTS.

TCA uptake kinetics of the other extracellular mutants C7A, C14A, C19A, and C106A was assessed in the presence and absence of CA-Asp−MTS to probe their possible involvement in bile acid−ASBT interaction. No change in K_T was observed in the presence of CA-Asp−MTS when compared to matching controls (Table 3) in the absence of the conjugate, for C7A, C19A, and C106A, suggesting that Cys residues 7, 19, and 106 do not play a critical role in protein−substrate interaction. On the other hand, C14A displayed a significant decrease in substrate affinity and J_{max} in the presence of the conjugate. This suggests that C14 may not be directly involved in ligand interaction, but could be located in the vicinity of a putative ligand binding region.

CA-Asp−MTS Inhibition of wt-hASBT ^{3}H-TCA Uptake Is Abrogated in the Presence of Cholic Acid. To ascertain the specificity of the interaction between bile acid−MTS conjugates and hASBT, protection of the bile acid-binding domain(s) in hASBT was established by preincubation with ligand. COS-1 cells transfected with wt-hASBT were pre-equilibriated (5 min) with increasing concentrations of cholic

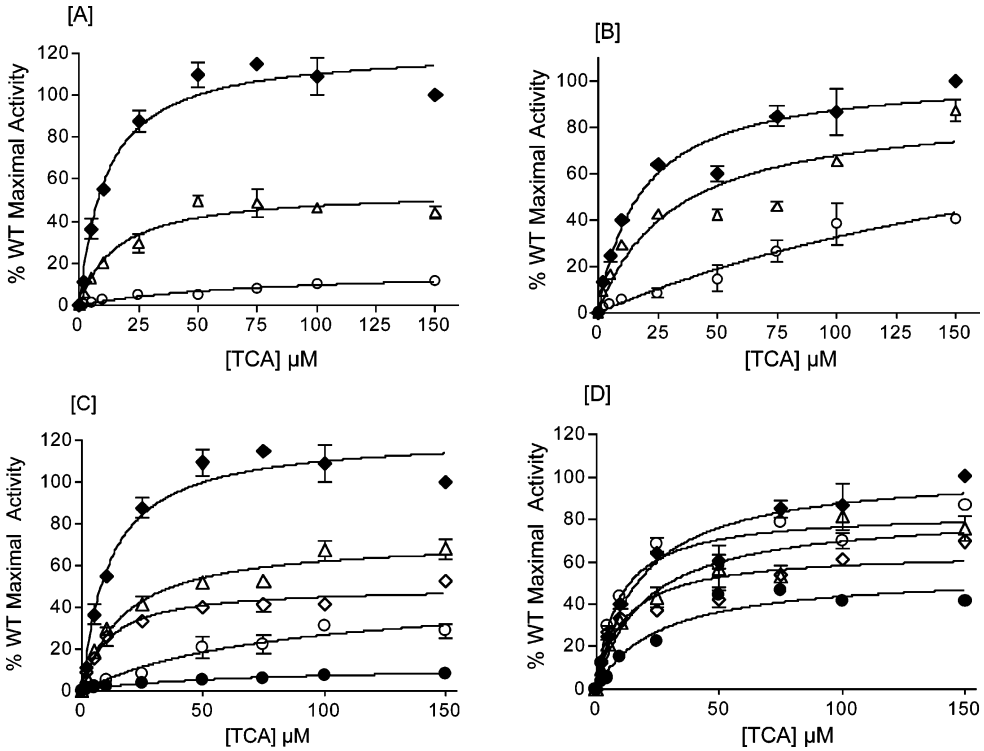

FIGURE 5: Inhibition studies of wild-type and C270A in the presence of MTSEA and bile acid−MTS conjugates: COS-1 cells transfected with wt-hASBT (A and C) and C270A (B and D). (A and B) After 48 h, cells were incubated for 10 min in the presence of 1mM MTSEA (△), 10mM MTSEA (○), and buffer (control) (◆). Treatment was followed by uptake kinetics at concentrations of taurocholic acid ranging from 0 to 150 μM. Uptake medium containing 137 mM NaCl was spiked with 5 μM ^{3}H-TCA (0.2Ci/mmol). Data were fitted to Michaelis−Menten equation, and curves represent best fits. (C and D) Kinetic constants for wt and C270A were determined in the presence of bile acid−MTS conjugates. COS-1 cells transiently transfected with wt (C) and C270A (D) were incubated with 1 mM of MTS-Asp (△), CA−MTS (●), CDCA-Asp−MTS (◇), CA-Asp−MTS (○), and buffer (◆) for 10 min, and their K_T and J_{max} values were determined by measuring uptake at varying concentrations of TCA in uptake medium spiked with 5 μM ^{3}H-taurocholic acid (0.2 Ci/mmol) for 12 min. Data were fitted to the Michaelis−Menten equation, and the curves represent the best fit with K_T values for WT and C270A, respectively, in the order of the aforementioned treatments. Each data point is represented as mean ± SD of three separate experiments and were considered statistically significant with $p \leq 0.01$

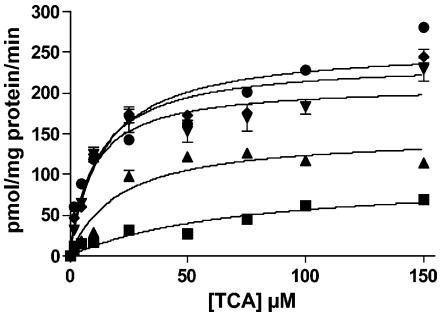

FIGURE 6: Protection of wt-hASBT from CA-Asp−MTS conjugate inhibition by cholic acid. COS-1 cells transfected with WT ASBT were preincubated (5 min) with 0 μM (■), 5 μM (▲), 50 μM (▼), and 100 μM (◆) cholic acid, prior to incubation with CA-Asp−MTS (1.0 mM) for 10 min at room temperature. Cells were washed and equilibrated with uptake medium and uptake kinetic parameters assessed as described in Materials and Methods. Control, wt-hASBT not treated with CA-Asp−MTS (●). Data were fitted to the Michaelis−Menten equation, and each data point is an average of two different experiments.

acid (0−100 μM) and exposed to CA-Asp−MTS (1.0 mM) for 10 min. At approximately 50 μM cholic acid, wt-hASBT uptake activity was restored to control values (cells not treated with CA-Asp−MTS) (Figure 6). These results demonstrate that the interaction of CA-Asp−MTS with hASBT is specific and that the presence of excess substrate abrogates alkylation of Cys residues in the transporter.

In all above experiments cell viability was consistently found to be greater than 95% as detected with ethidium bromide and calcein-AM (Molecular Probes Inc., Eugene, OR) (data not shown).

DISCUSSION

In the present study we sought to define a strategy for enabling SCAM studies in hASBT in the presence of native Cys residues. A functional role of Cys residues in ASBT has been suggested previously (*10*, *11*, *21*), and as shown in the present study, modification of certain Cys residues renders the protein inactive. Although SCAM studies generally require a Cys-less protein, this strategy cannot be employed to hASBT.

First, mutation of all indigenous Cys residues to either Ala or Thr was carried out to identify those residues that may play a critical role in hASBT function (Table 2). C51, C105, C132 (131-*NTCP*), and C255 (254-*NTCP*) are strongly conserved between ASBT and NTCP (Figure 1), suggesting their intricate involvement in hASBT function. This is supported by the observation that substitution of these residues produces loss-of-function mutants (Table 2). Similar results were observed with C51 mutations of the mouse ortholog of ASBT (*11*). However, the direct involvement of loss-of-function Cys mutants (C51A/T, C74A/T, C105A/T, C144A) in substrate interaction cannot be ruled out based on the present data and warrants further investigation.

Substrate transport is abrogated in mutants C74A/T (Table 2) as a result of defective cell surface protein expression (Figure 3). Hence, we propose that C74 may play a role in maintaining the structural integrity of the transporter and/or play a role in cell surface trafficking. In general, Ala substitutions at C14, C106, C132, C255, and C270 resulted in significantly higher ligand uptake compared to Thr mutants at these same positions (Table 2). This is consistent with previous data on *lac* permease demonstrating that small hydrophobic side chains (Ala, Val) generally increase the apparent affinity of permease for substrate, while hydrophilic side chains (Ser, Thr, Asp) decrease apparent affinity (*22*). The opposite effect was observed for C144, which cannot be explained by this general concept.

Our data indicate (Figure 4) that wt hASBT is strongly inhibited in the presence of each individual MTS reagent. This suggests that these agents modify one or more native Cys residues that may (1) lie in the ligand translocation pathway or (2) indirectly affect ligand transport. In general, extracellular Cys residues exhibit increased susceptibility to polar MTS reagents. To investigate this possibility, we focused our next experiments on functionally active, extracellularly located mutants (i.e., C7, C14, C19, C106, and C270; Table 2). Interestingly, substrate transport in mutant C270A was not significantly inhibited in the presence of polar MTS reagents, whereas mutant C7A was decreased by merely 35%. Combined with the observation that all other extracellular mutants are susceptible to polar MTS reagents, this suggests that C270 and C7 may be responsible for the observed loss of functional activity of the other mutants. Alternatively, C270 and C7 may be the only residues that significantly impact ligand translocation upon modification. Previously, we have shown that pairwise mutations C270N and Q268S successfully introduced a N-glycosylation consensus sequence (*3*). According to the 7 TM toplogy of hASBT, these residues are located on EL3, a relatively long and hydrophilic loop connecting TM domains 6 and 7. Since N-glycosylation of a membrane protein occurs only on the extracellular side of the plasma membrane, combined with the present findings, this lends further support for the exofacial localization of C270 in a highly solvent accessible region of extracellular loop 3 (Figure 2) (*3*).

Thiol-specific modifiers, such as the MTS reagents, have been applied successfully to study the structure and function of many membrane transporters (*23*−*26*). However, these agents generally modify *all* accessible Cys residues and do not effectively identify those that may be located within the substrate translocation pathway. To enhance probe specificity, we custom-designed MTS−bile acid conjugates by coupling MTS to cholic acid using an aspartate spacer. These novel conjugates were subsequently incubated with several hASBT mutants to determine their functional significance (Figure 5, Table 3). Their specificity was verified by preincubation of wt hASBT with cholic acid to protect the protein from conjugate labeling (Figure 6). Our data show that substrate protection of hASBT labeling occurs in a concentration-dependent fashion, thereby suggesting probe specificity. Further characterization of the extracellular Ala mutants showed that C7A, C19A, and C106A were not significantly affected by CA-Asp−MTS (Table 3), suggesting that these residues may not be located in the vicinity of the substrate binding region. On the other hand, unique kinetics of C270A in the presence of CA-Asp−MTS and other MTS−bile acid analogues (Figure 5D), suggests that this residue may be located in the vicinity of bile acid interacting region(s). Thus, our data corroborate earlier suggestions (*14*, *27*) that C270 is not involved in protein−ligand interactions but is probably located in close proximity to the binding region. Combined with our finding that C255A constitutes a loss-of-function mutant, this may suggest that EL3 plays a critical role in substrate recognition.

In conclusion, we have demonstrated that (i) multiple Cys residues are essential for hASBT function, (ii) C74 may be critical for the proper folding and/or targeting of the transporter to the cell surface, and (iii) C270A in combination with bile acid−MTS conjugates can aid in defining the putative ligand binding region(s) and translocation pathway. We also show that the C270A mutant can be used as a scaffold for future cysteine-scanning mutagenesis as this mutant is least sensitive to the polar MTS reagents. Furthermore, these conjugates may be used as attractive tools for characterizing other bile acid transporters such as hepatic *NTCP* and the bile salt excretory pump (*BSEP*).

ACKNOWLEDGMENT

The authors would like to thank Dr. Vanessa M. D'Souza for her valuable scientific suggestions and proofreading of the manuscript.

REFERENCES

1. Craddock, A. L., Love, M. W., Daniel, R. W., Kirby, L. C., Walters, H. C., Wong, M. H., and Dawson, P. A. (1998) Expression and transport properties of the human ileal and renal sodium-dependent bile acid transporter, *Am. J. Physiol. 274*, G157−G169.
2. Oelkers, P., Kirby, L. C., Heubi, J. E., and Dawson, P. A. (1997) Primary bile acid malabsorption caused by mutations in the ileal sodium-dependent bile acid transporter gene (SLC10A2), *J. Clin. Invest. 99*, 1880−1887.
3. Zhang, E. Y., Phelps, M. A., Banerjee, A., Khantwal, C. M., Chang, C., Helsper, F., and Swaan, P. W. (2004) Topology scanning and putative three-dimensional structure of the extracellular binding domains of apical sodium-dependent bile acid transporter, *Biochemistry 43*, 11380−11392.
4. Hallen, S., Branden, M., Dawson, P. A., and Sachs, G. (1999) Membrane insertion scanning of the human ileal sodium/bile acid co-transporter, *Biochemistry 38*, 11379−11388.
5. Izzat, N. N., Deshazer, M. E., and Loose Mitchell, D. S. (2000) New molecular targets for cholesterol-lowering therapy, *J. Pharmacol. Exp. Ther. 293*, 315−320.
6. Thompson, G. R., and Naumova, R. P. (2000) Novel lipid-regulating drugs, *Expert Opin. Invest. Drugs 9*, 2619−2628.
7. Mueckler, M., and Makepeace, C. (2004) Analysis of transmembrane segment 8 of the GLUT1 glucose transporter by cysteine-scanning mutagenesis and substituted cysteine accessibility, *J. Biol. Chem. 279*, 10494−10499.
8. Chen, J. G., Liu-Chen, S., and Rudnick, G. (1997) External cysteine residues in the serotonin transporter, *Biochemistry 36*, 1479−1486.
9. Mueckler, M., and Makepeace, C. (2002) Analysis of transmembrane segment 10 of the Glut1 glucose transporter by cysteine-scanning mutagenesis and substituted cysteine accessibility, *J. Biol. Chem. 277*, 3498−3503.
10. Kramer, W., Nicol, S. B., Girbig, F., Gutjahr, U., Kowalewski, S., and Fasold, H. (1992) Characterization and chemical modification of the Na (+)-dependent bile-acid transport system in brush-border membrane vesicles from rabbit ileum, *Biochim. Biophys. Acta 1111*, 93−102.
11. Saeki, T., Kuroda, T., Matsumoto, M., Kanamoto, R., and Iwami, K. (2002) Effects of Cys mutation on taurocholic acid transport by mouse ileal and hepatic sodium-dependent bile acid transporters, *Biosci., Biotechnol., Biochem. 66*, 467−470.

12. Blumrich, M., and Petzinger, E. (1990) Membrane transport of conjugated and unconjugated bile acids into hepatocytes is susceptible to SH-blocking reagents, *Biochim. Biophys. Acta 1029*, 1−12.
13. Blumrich, M., and Petzinger, E. (1993) Two distinct types of SH-groups are necessary for bumetanide and bile acid uptake into isolated rat hepatocytes, *Biochim. Biophys. Acta 1149*, 278−284.
14. Hallen, S., Fryklund, J., and Sachs, G. (2000) Inhibition of the human sodium/bile acid cotransporters by side specific methanethiosulfonate sulphydryl reagents: substrate controlled accessibility of Se of activation, *Biochemistry 39*, 6743−6570.
15. Loo, T. W., and Clarke, D. M. (2001) Defining the drug-binding site in the human multidrug resistance P-glycoprotein using a methanethiosulfonate analog of verapamil, MTS-verapamil, *J. Biol. Chem. 276*, 14972−14979.
16. Loo, T. W., Bartlett, M. C., and Clarke, D. M. (2003) Methanethiosulfonate derivatives of rhodamine and verapamil activate human P-glycoprotein at different sites, *J. Biol. Chem. 278*, 50136−50141.
17. Guan, L., Sahin-Toth, M., Kalai, T., Hideg, K., and Kaback, H. R. (2003) Probing the mechanism of a membrane transport protein with affinity inactivators, *J. Biol. Chem. 278*, 10641−10648.
18. Wong, M. H., Oelkers, P., and Dawson, P. A. (1995) Identification of a mutation in the ileal sodium-dependent bile acid transporter gene that abolishes transport activity, *J. Biol. Chem. 270*, 27228−27234.
19. Frillingos, S., Sahin-Toth, M., Wu, J., and Kaback, H. R. (1998) Cys-scanning mutagenesis: a novel approach to structure−function relationships in polytopic membrane proteins, *FASEB J. 12*, 1281−1299.
20. Holmgren, M., Liu, Y., Xu, Y., and Yellen, G. (1996) On the use of thiol-modifying agents to determine channel topology, *Neuropharmacology 35*, 797−804.
21. Baringhaus, K. H., Matter, H., Stengelin, S., and Kramer, W. (1999) Substrate specificity of the ilieal and hepatic Na+/bile acid cotransporters of the rabbit. II. A reliable 3D QSAR pharmacophore model for the ileal Na+/bile acid transporter, *J. Lipid Res. 40*, 2158−2168.
22. Jung, H., Jung, K., and Kaback, H. R. (1994) Cysteine 148 in the lactose permease of *Escherichia coli* is a component of a substrate binding site. 1. Site-directed mutagenesis studies., *Biochemistry 33*, 12160−12165.
23. Kanaya, E., Kanaya, S., and Kikuchi, M. (1990) Introduction of a non-native disulfide bridge to human lysozyme by cysteine scanning mutagenesis, *Biochem. Biophys. Res. Commun. 173*, 1194−1199.
24. Kulkarni, A. A., Haworth, I. S., and Lee, V. H. (2003) Transmembrane segment 5 of the dipeptide transporter hPepT1 forms a part of the substrate translocation pathway, *Biochem. Biophys. Res. Commun. 306*, 177−185.
25. Loo, T. W., Bartlett, M. C., and Clarke, D. M. (2004) Disulfide cross-linking analysis shows that transmembrane segments 5 and 8 of human P-glycoprotein are close together on the cytoplasmic side of the membrane, *J. Biol. Chem. 279*, 7692−7697.
26. Cao, W., and Matherly, L. H. (2004) Analysis of the membrane topology for transmembrane domains 7−12 of the human reduced folate carrier by scanning cysteine accessibility methods, *Biochem. J. 378*, 201−206.
27. Hallen, S., Bjorquist, A., Ostlund-Lindqvist, A. M., and Sachs, G. (2002) Identification of a region of the ileal-type sodium/bile acid cotransporter interacting with a competitive bile acid transport inhibitor, *Biochemistry 41*, 14916−14924.

BI050553S